URTeC: 1922149

Horizontal Lateral Image Analysis Applied to Fracture Stage Optimization in Eastern Barnett Shale, Tarrant and Dallas Counties, Texas

T. N. Olsen *[1]; M. P Germinario [1]; R. Reinmiller [2]; D. Martinez[2]; R. L. Parker[2]
[1] Beacon E&P, Denver, CO, United States. [2] Task-Fronterra Geoscience, Denver, CO, United States

This paper was prepared for presentation at the Unconventional Resources Technology Conference held in Denver, Colorado, USA, 25-27 August 2014.

Abstract

The “core” region of the Barnett Shale play in eastern Tarrant and western Dallas Counties, Texas, has prime development potential. This stems from a combination of maximum target thickness of 450’ to 500’ and a thick Viola Limestone, affording a significant barrier to Ellenberger water production. Structural complexity increases approaching the Ouachita Thrust belt to the east, as reflected in increased variability in Barnett natural fractures and rock stress properties.

Borehole image logs from 3 horizontal wells in the Barnett reveal significant variability in natural fracturing, faults and drilling induced fracture distribution along their laterals. The presence or absence of drilling induced transverse and longitudinal fractures can be directly linked to the changes in frac gradient and proppant placement during the fracture treatments and flowback response. A geomechanical study of all 3 wells identified the geometry of critically-stressed fractures and faults. Variation in differential stress along the lateral and changes in the geometry of critically-stressed fractures and faults can significantly alter the induced hydraulic fracture response (complex vs. planar fractures) in these stages, ultimately governing production response.

We developed criteria to use drilling induced fracture patterns from horizontal borehole image data to optimize the fracture stage design, custom fitting the stimulation to lateral changes in stress anisotropy.

From production histories, we show that stage-by-stage modification of the pump-ins, accommodating borehole image log-derived information, was able to improve frac efficiency and EUR, even in highly fractured laterals.

Barnett Shale Stimulation Overview

History: For many years operators have been intrigued by the high mud log gas shows that occurred when penetrating the Barnett shale formation. However, the extremely low permeability inhibited any economic exploitation. During the late 1980s and the 1990s, successful economic development of unconventional sources of natural gas in coal seams became widespread, often through fracture stimulation. A common characteristic of these economic coal seams were high gas shows in the mud logs. The success of the Unconventional CBM caused innovative operators to revisit other formations where high gas shows were seen in mud logs. George P Mitchell began attempting to exploit the Barnett formation by stimulating the rock with sand and high-viscosity crosslink gel fracturing fluids. This was successful in producing gas from the formation, but the economics were marginal at best. Later attempts were made to re-fracture some of these wells, only this time the stimulation fluid was a thin water system that contained only a friction reducer. This resulted in significant additional production over the original fracture stimulations, and the reduced cost of the slickwater fluids enabled much larger volumes of fluid to be used. A relatively newly commercial technique, called Microseismic mapping, uses highly sensitive acoustic listening devices in an offsetting wellbore to hear and locate acoustic events associated with induced hydraulic fracturing. This Microseismic mapping technique was used to monitor some of these slickwater re-fracs. The mapping revealed a surprising result: instead of the traditional single fracture plane, the slickwater fracturing fluid was creating a complex multi-planar fracturing system. Eventually the slickwater fracturing in the Barnett was applied to horizontal wells and to multi-stage fracturing technology and the Barnett was transformed into a major economic gas resource.

Rock Properties and Stimulation- The highly siliceous composition of the target benches of the Barnett formation makes for a very brittle rock. This brittleness and, in particular, the very low Poisson's Ratio of the rock, enable multiple planar complex fracture systems. The complex fracturing creates huge volumes of contact area to the formation. The term "Stimulated Rock Volume" or SRV has been coined to describe the stimulated surface area created by complex fracturing. A large SRV enables economic production rates despite the nano-darcy permeability typical of the Barnett rock matrix. Several publications have documented the mechanism of complex fracturing by the use of thin slickwater fracturing fluids (Ketter, 2008; Warpinski, et al., 2005; Warpinski,et al., 1987) to name a few.

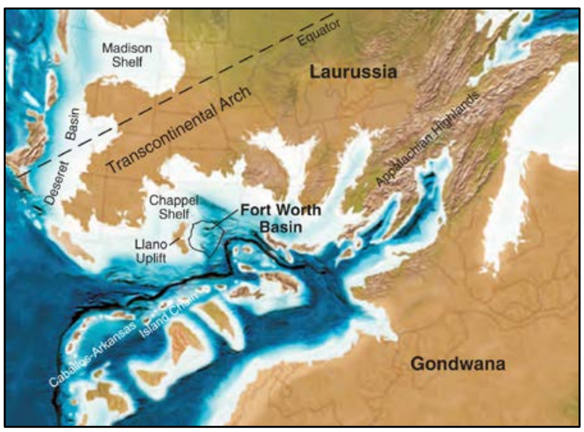

Figure 1: Regional paleogeography of the southern mid-continent during Late Mississippian (325 Ma), showing approximate location of the Fort Worth Basin. Modified from Blakey, 2005, Bruner and Smosna, 2011.

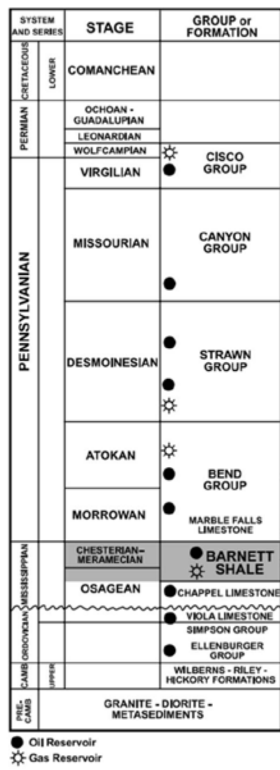

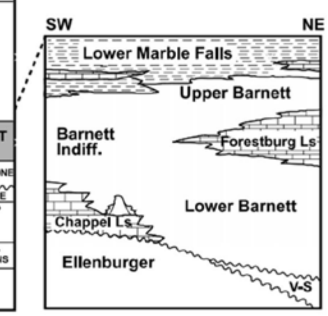

Figure 2: Generalized stratigraphic column, Fort Worth Basin Barnett shale is shaded. Expanded section (right) shows details of the Mississippian stratigraphy. V-S refers to the Viola –Simpson interval. Modified from Montgomery and others, 2005.

Induced hydraulic fracturing consists of two main rock failure mechanisms. Tensile failure first propagates in the direction of the maximum horizontal stress. Tensile fractures are caused by the hydraulic pressure from the water injected into the rock. The hydraulic pressure acts like a wedge and literally parts the formation. Shear fracturing can occur secondarily in planes outside that of the maximum horizontal stress, often along pre-existing planes of weakness within the structure of the rock. Shear fracturing occurs in association with the primary tensile fracturing and occurs when rock undergoes shear forces. When shear failure occurs, there is a micro-displacement in the rock. Generally, shear fractures have very little width, so the majority of the fracture fluid and sand volume exists within the tensile fractures. Under certain circumstances, when the rock Poisson's ratio is very low and the horizontal stress anisotropy is also low, tensile fracturing can occur in multiple planes (Olsen et al, 2009). Under these conditions, frac fluid and proppant can be transported in multiple fracture planes. A formation where multi-planar proppant placement occurs will have a very different SRV geometry than a formation where only planar proppant transport occurs. A single plane-propped fracture creates a much longer and a much narrower SRV than a formation with multi-planar proppant placement.

Knowing what type of stimulation will occur in a well would allow significant modifications to the stimulation design to optimize the stimulation. For example: if you knew you had multi-planar proppant placement, fewer stages would be required to stimulate the entire lateral. Larger volumes could be pumped per stage at higher pump rates and a higher percentage of smaller mesh proppant would be used. Conversely a planar-propped formation would require more frac stages per lateral but smaller volumes and lower pump rates each stage.

Image logs and/or modern sonic logs can be used to help determine the properties of the formation and how it will stimulate. Knowing this information and acting to modify the stimulation programs accordingly, can help either reduce stimulation costs or increase the stimulation effectiveness.

Fort Worth Basin Barnett Shale Overview -

The Fort Worth Basin (FWB) was formed during the late Paleozoic Ouachita Orogeny by the convergence of Laurussia and Gondwana (Figure 1). The FWB is depicted in paleographic reconstructions as a narrow, restricted, inland seaway (Gutschick and Sandburg, 1983; Blakely, 2005). Figure 2 illustrates the generalized stratigraphic column from the Fort Worth Basin, highlighting the Mississippian. Figure 3 shows the stratigraphic relations in the greater FWB, regional structural elements and the location of the study area. In the FWB, the Barnett Shale ranges from 50’ to over 1000’ thick; in the study area the Barnett thickness ranges from 450’ to 500’ (Figure 5).

Barnett lithology is dominated by black, organic-rich, laminated, siliceous mudstone mixed with laminated, argillaceous lime mudstones and argillaceous lime packstones (Loucks and Ruppel, 2007). Silica generally comprises 35-50% of the formation by volume and clay minerals are usually less than 35%. There is a highly variably carbonate content (Figure 4).

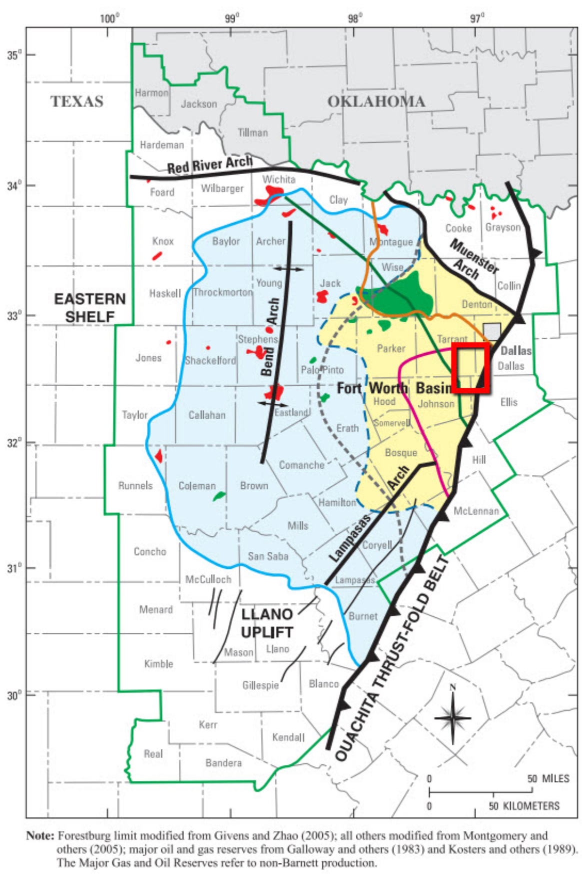

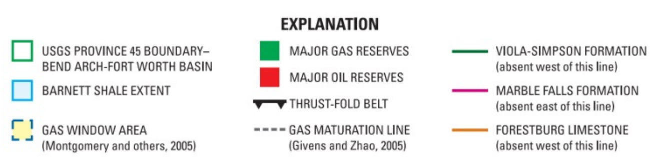

Figure 3: Extent of the Barnett Shale in the Fort Worth Basin:

(A) Pinch out of the Forestburg Limestone member in orange.

(B) Pinch out of the underlying Viola-Simpson Formations in dark green.

(C) Pinch out of the overlying Marble Falls Formation in pink.

Red box indicates the study area of this paper. Modified from Barnett Shale Maps, 2007 and Bruner and Smosna, 2011.

The total organic carbon (TOC) of the Barnett shale in the FWB ranges from 2-6%. The thermal maturities of the Barnett range from 0.7 to 1.7 R_o. The FWB has undergone a complex burial history with multiple thermal events (Pollastro et al., 2003 and Montgomery, 2005). The Barnett's relatively high brittleness is attributed to the

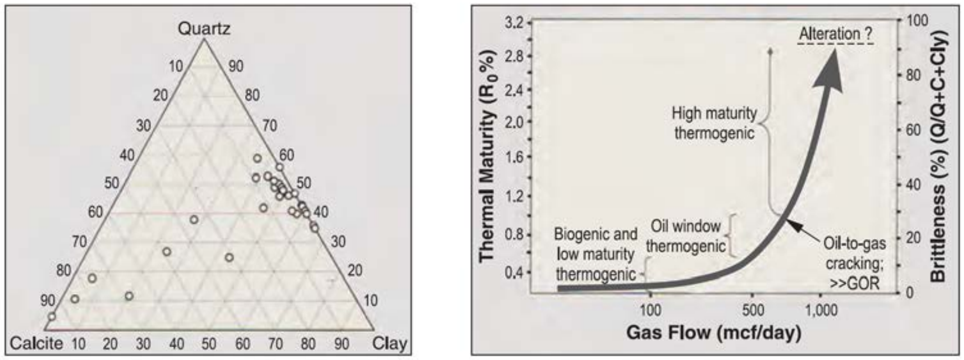

Figure 4: Left: This ternary diagram displays the mineral content of the Barnett Shale in terms of quartz, clay minerals and calcite. Right: This graph depicts the relationship between gas flow, thermal maturity and shale brittleness. Modified from Jarvie and others, 2007; Bruner and Smosna, 2011.

combination of high silica content and high thermal maturity (Figure 4) (Jarvie et al., 2007)

Many workers have studied the various aspects of the Barnett Petroleum system. Details on the Barnett depositional system, lithology, geochemistry and FWB petroleum geology can found in Bruner and Smosna, 2011; Bowker, 2002; Browning and Martin, 1982; Gale, et al., 2007; Hickey and Henk, 2007; Hill et al. 2007, Jarvie et al., 2004; Jarvie et al., 2007; Loucks and Ruppel, 2007; Montgomery et al., 2005; Martineau, 2007; Papazis, 2005; Pollastro et al.,2003; Pollastro, 2007 and Slatt et al., 2009.

Regional Stresses - Natural fracturing

The FWB is associated with large scale structural features. Most notable are the Muenster Arch and the Ouachita Fold and Thrust belt (Figure 3). These structures are generally associated with the late Paleozoic Ouachita Orogeny. For the FWB, published data from the World Stress Map (Tingay, 2006), indicates that present-day S_{Hmax} is oriented NE-SW. This trend is consistent with the orientation of drilling-induced fractures observed in borehole image log data in vertical Barnett wells (Figure 5, right). Natural fractures found in the Barnett shale are predominantly healed with calcite cement and are likely to be reactivated as pre-existing zones of weakness during the hydraulic fracturing process (Bowker, 2007; Gale et al, 2007). Work with core and borehole image logs has documented the existence of two sets of natural fractures. One fracture set strikes NE-SW, coincident with the regional $S_{Hmax.}$ The other fracture set strikes E-W with some scatter (Gale et al., 2007). The mechanisms for the formation of these healed natural fractures may be related to the large structural features surrounding the basin, but the complex structural and burial history of the basin suggests that there may be multiple mechanisms responsible for the fracture formation.

Eastern Central Barnett Play – Core Dry Gas Area

This discussion will focus on well data and completions from 3 horizontal wells in the most eastern part of the central core of the Barnett dry gas play. The 3 subject wells are the Palomino 9H (Pal 9H) the Thoroughbred 2H (TB 2H) and the SE Mansfield 12H (SEM 12H). The Pal 2H & TB 2H are located just north of Interstate 30 in westernmost Dallas County. SEM 12H is located 14.6 miles to the SSW, in the southeastern corner of Tarrant County (Figure 5). These wells all had horizontal micro-resistivity logs run in the laterals. The type log for the area from the Pal 9H pilot (Figure 6) illustrates a Barnett that is 467' thick. The calculated Target Zone Index curve (TZI) identifies the most siliceous portion of the section using simple porosity curves (neutron porosity minus density porosity, 2.71 matrix). Coupled with the FLEX mineralogy analysis, the indicated target zone has the highest silica content, therefore has the highest brittleness and the best potential for complex fracturing during the hydraulic stimulation.

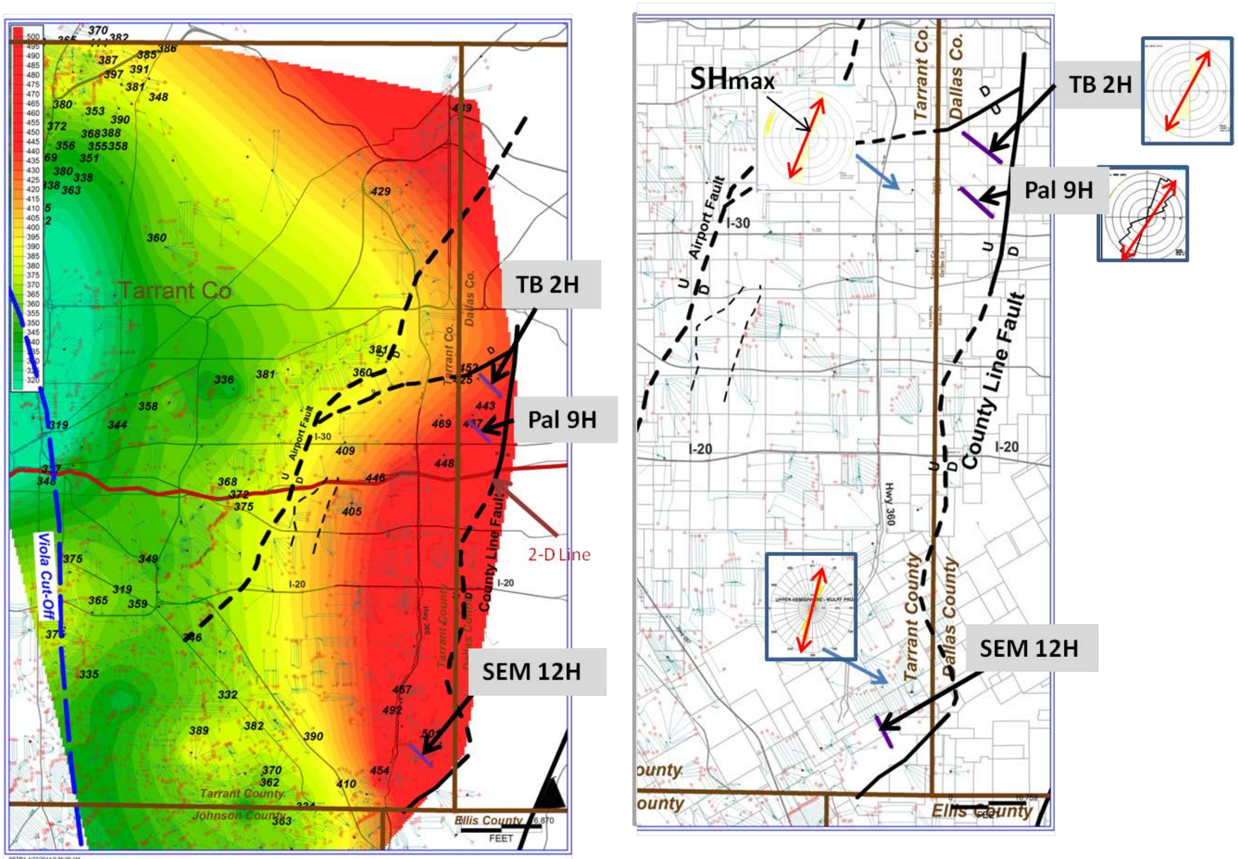

Figure 5: Left: Isopach of total Barnett thickness from pilot well control for SW Tarrant County. Right: Wulff plots indicating SHmax from interpreted from drilling Induced fracture analysis on vertical pilot holes. The well locations described in this paper are noted on both maps.

Local Structural Issues

The Pal 9H and TB 2H wells are situated in a unique structural setting. In westernmost Dallas and eastern Tarrant Counties, two major Ouachita-related structural features exert a strong influence on the geometry of the subsurface. First, the presence of a significant normal fault system is revealed by both 2-D and 3-D seismic coverage and is verified by well control. The prominent 1000'+ down-to-the-east, high-angle normal fault is termed the ***County Line Fault*** for the purposes of this paper (Figures 5 and 7). Overriding, and truncating, this normal fault is the second feature: a thrust sheet comprised of deformed Atokan-aged strata. At the Pal 9H and TB 2H wells, the Barnett shale is positioned in the footwall and is undisturbed. Dipmeter logs, acquired from pilot holes drilled in the area, place the thrust fault 200' to 400' above the Barnett. This structural setting is likely to contribute to variability in stress anisotropy noted from lateral and completions results from both the TB 2H and the Pal 9H. The area of the SEM 12H well, 14.6 miles to the SSW, is unaffected by these thrusted Atokan features, exhibiting a more uniform stress anisotropy.

Borehole Resistivity Imaging

Borehole resistivity image logs provide high-resolution control on the distribution and geometry of faults, fractures and present-day stress indicators in the three lateral wells included in this study. The discussion of image log data that follows compares and contrasts the features identified across the three laterals. These observations identify the total number of fractures, fracture strike trends, the geometry of critically-stressed fractures and faults and the trajectory of near wellbore stresses. As displayed in Figure 8, fractures were identified in the SEM 12H from a measured depth of 8,800'to 12,460' (3,660' total). There were 889 fractures in the SEM 12H and a vast majority of these fractures were >70° in dip magnitude. The fracture strike trend is strongly NE-SW and is aligned with S_{Hmax}. In addition to fractures, 3 faults were identified in the SEM 12H. Over the length of the entire image dataset, the wellbore displays an average fracture spacing of 1 fracture every 4.1 feet.

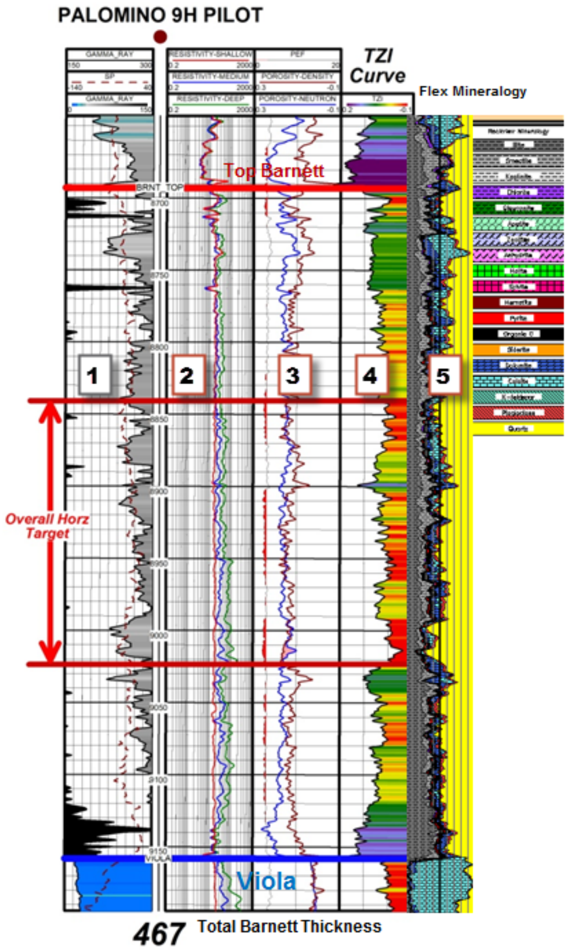

Figure 6: Barnett type log for westernmost Dallas County. Palomino 9H (Pal 9H on index map).

Curves: 1- Gamma ray. 2- Deep-shallow induction curves. 3- Density neutron porosity curves with PEF. 4- Calculated TZI curve. 5 - FLEX mineralogy

Figure 9 displays the fracture characteristics of the TB 2H lateral, which ranges in measured depth from 9400' to 14760' (5,360' total). In contrast to the SEM 12H, this lateral displays 2 prominent fracture strike directions and a large increase in the total number of fractures (n=1330). The dominant strike trend is oriented E-W and is almost exclusively comprised of cemented fractures (indicated by the magenta rose petals). This dominant strike trend has a greater tendency to dip to the N (indicated by a clustering of poles to planes in the S part of the lower hemisphere projection). The secondary fracture strike direction is oriented NNE-SSW and is dominated by closed fractures, which are typically lower angle (>70°) and dip preferentially to the ESE. In addition to the fractures, 16 faults were identified in the TB 2H. The 5,360' of the lateral averages a fracture density of 1 fracture every 4' - very similar to the SEM 12H.

Figure 10 displays the fracture characteristics from the measured depth range of 9170' to 14651' (5,481' total) in the Pal 9H. With 3,451 fractures, this is the most fractured well of the 3 laterals in this study (and is one of the most highly fractured wells known from the area). A strongly dominant fracture strike trend is oriented E-W with dips to both the N and S. The majority of these fractures are cemented. A secondary fracture strike direction is oriented NNE-SSW (aligned with S_{Hmax}) and is dominated by a comparatively large number (n=874) of open fractures. The open fractures represent 24% of the total fracture population. There were 16 faults identified in the lateral. High-angle fractures (>70°) are most abundant, as indicated in the dip angle histogram (bottom left). Across the lateral length of the Pal 9H (5,481'), the average fracture spacing is 1 fracture for every 1.6'. Although the Palomino 9H and the Thoroughbred 2H are less that 2 miles apart, and both exhibit similar fracture strike trends, the Pal 9H has almost 3 times the number of fractures.

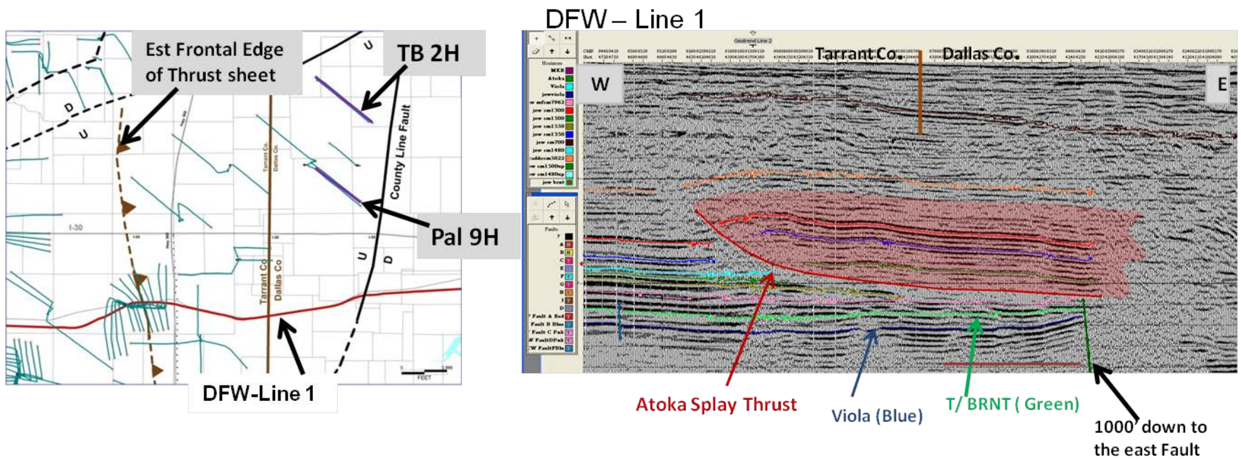

Figure 7: Left: Index map showing the location of the DFW Line 1 and the estimated frontal edge of the Atoka Splay Thrust. Right: Interpreted 2-D Seismic line DFW Line 1 illustrating the Atoka Thrust plat overriding an undisturbed Barnett Section.

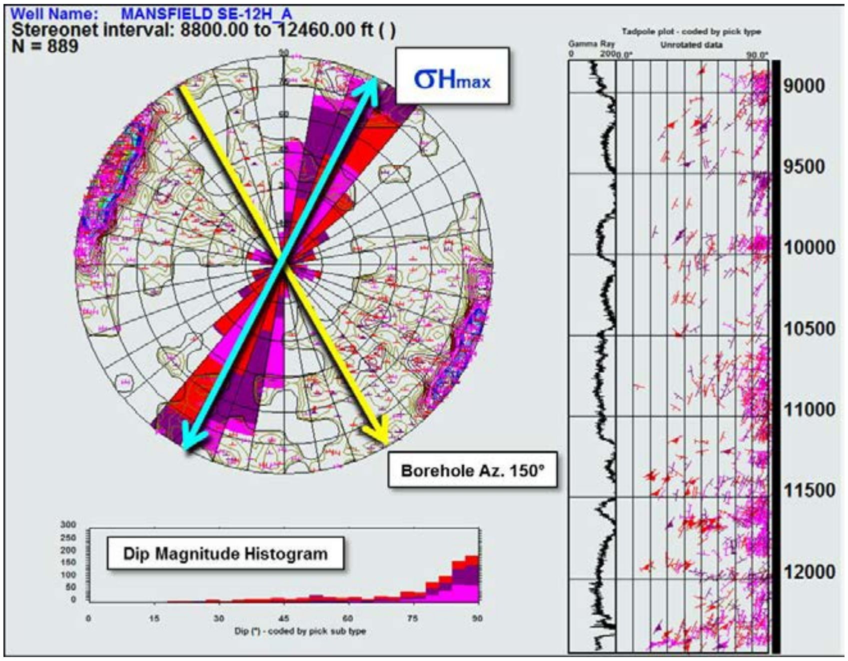

Figure 8: The diagram above displays the geometric characteristics of the fractures identified in the SE Mansfield 12H (SEM 12H) from a measured depth of 8,800'to 12,460' (3,660' total). The lower hemisphere stereonet (Schmidt net, upper left) displays fracture strikes as rose petals and poles to fracture planes as strike and dip symbols. Poles to fracture planes are contoured to accentuate clustering. The diagram at lower left displays fracture dip angle (from 0° to 90°, x-axis). Fracture symbols on this tadpole plot are aligned with strike and point in the direction of dip. Figures 9 and 10 are similarly styled.

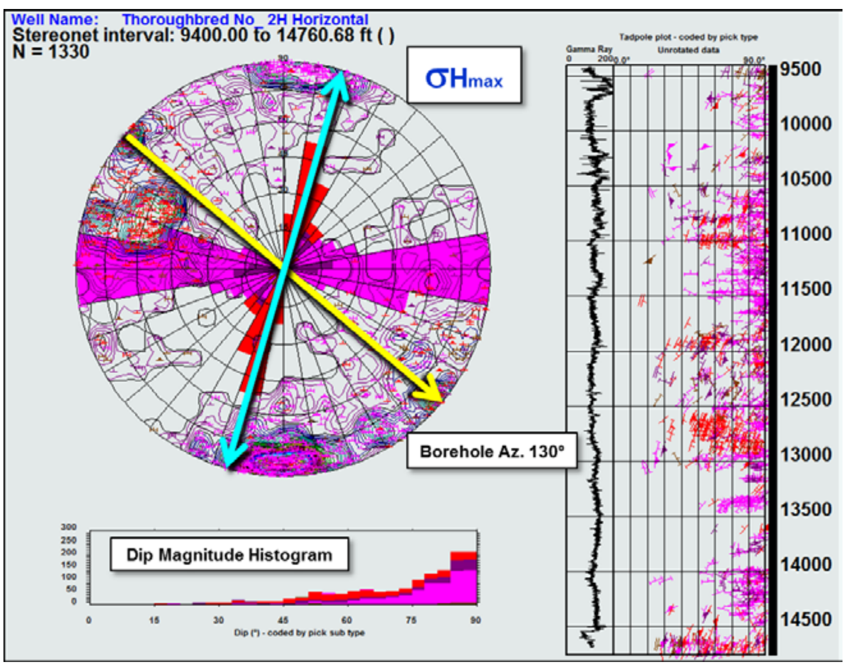

Figure 9: The diagram above displays the geometric characteristics of the fractures identified in the TB 2H from a measured depth of from 9400' to 14760' (5,360' total). This diagram is constructed in a style similar to that of Figure 8

Geomechanics and In situ Stress Characterization

When a well is drilled in a formation, solid materials are removed and replaced with drilling fluid (Figure. 11). Because the well fluid pressure does not match the stress exerted by the removed solid, there will be an alteration in the stress-state of the formation around the well resulting in wellbore stress concentration. Under a normal stress regime, stress concentration can create drilling induced longitudinal and transverse fractures which reveal information about the far field stresses. In a lateral borehole, assuming that certain parameters are within a reasonably constant range (e.g., wellbore deviation, pore pressure, rock strength properties, overburden, and operational parameters), the appearance of the drilling-induced fractures in the image log data can be used to qualitatively estimate changes of the far field stresses along the borehole trajectory.

Figure 12 is a snapshot illustrating the appearance of longitudinal and transverse fractures from the TB 2H at two depth intervals. Assuming that a wellbore is drilled parallel or sub-parallel to the minimum horizontal stress (S_{hmin}) direction, transverse fractures will develop in intervals characterized by a lower value of S_{hmin} (and hence, a greater likelihood of horizontal stress anisotopy). In such a case, (figure 12, ~11094') the resultant hydraulic fracture fairway would be long and narrow. Portions of a borehole characterized by both longitudinal and transverse fractures (Figure 12, ~8,942') are typified by lower horizontal stresses (both S_{hmin} and S_{Hmax} decrease resulting in a lesser degree of anisotropy), with a resulting hydraulic stimulation fracture fairway that would be shorter and wider. If no induced fractures are seen, the horizonal stresses are high, fracture intiation will be high, and the anisotropy relation is somewhat inconclusive. (G. Waters SPE 103232).

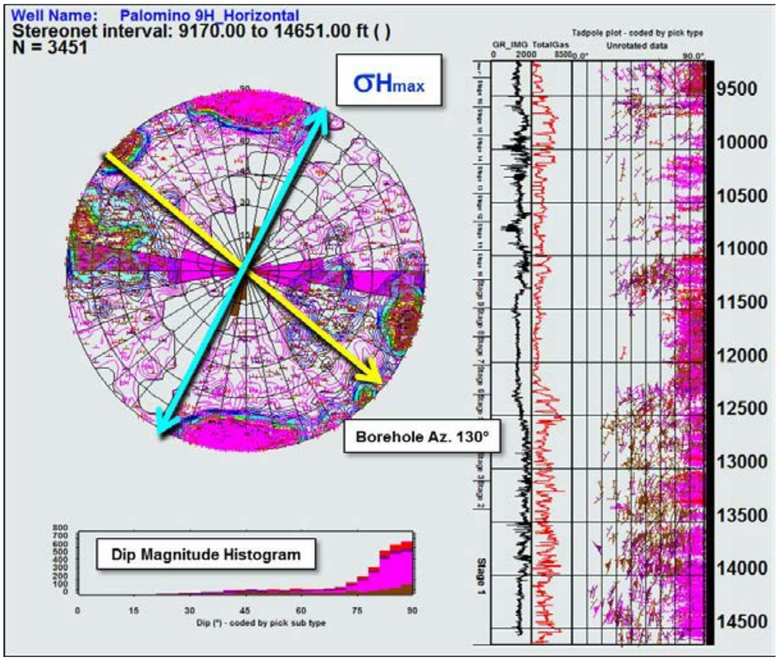

Figure 10: The diagram above displays the geometric characteristics of the fractures identified in the Pal 9H from a measured depth of 9170' to 14651' (5,480' total). This diagram is constructed in a style similar to that of Figure 8.

SEM 12H Near Wellbore Stress

Present-day stress characteristics of the 3 wells, determined from analysis of horizontal resistivity image log data, is presented in the next several diagrams. Each diagram is designed with a similar style. The significant data tracks are identified by the numbers 1 through 7 on Figure 13, which are delineated from right to left, as follows:

1. The numbers indicate the fracture gradient for each stage.
2. The curve is a graphical representation of the fracture gradient values.
3. The bars indicate the position of faults identified by image logs along the lateral.
4. The blue peaks represent the density of fractures per linear foot, averaged by a sliding 10' window.
5. The green bars indicate the position of transverse induced fractures identified by image log analysis.
6. The red bars indicate the position of longitudinal induced fractures identified by image log analysis.
7. The resistivity image log for the horizontal borehole.

The SEM 12H well (Figure 13) exhibits transverse and longitudinal fractures thoughout the entirety of the lateral borehole. The fracture frequency curve displays swarms of fractures and the strikes of these fractures are almost uniformly aligned with S_{Hmax}. The fracture gradient ranges from 0.73 to 0.84, with an average value of 0.77. This

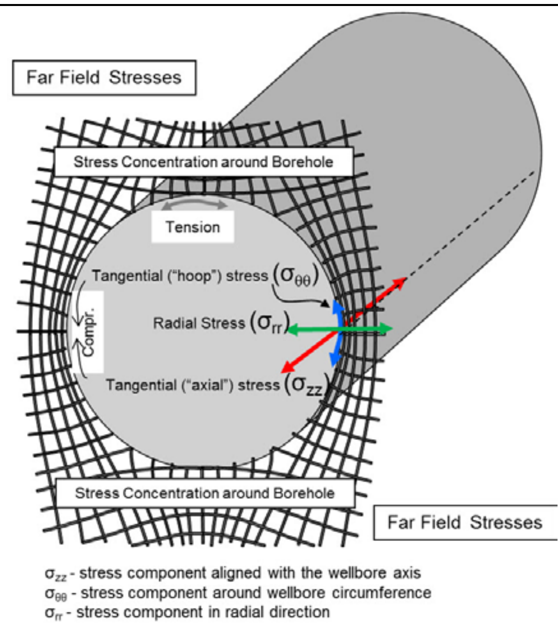

Figure 11: Wellbore stress distribution.

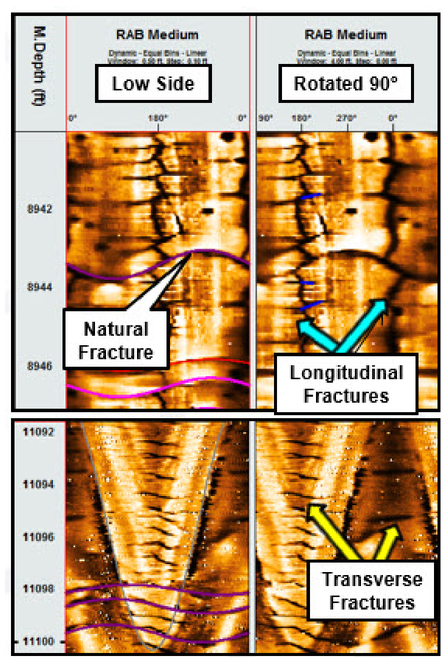

Figure 12: Snapshot of the longitudinal and transverse fractures in TB.

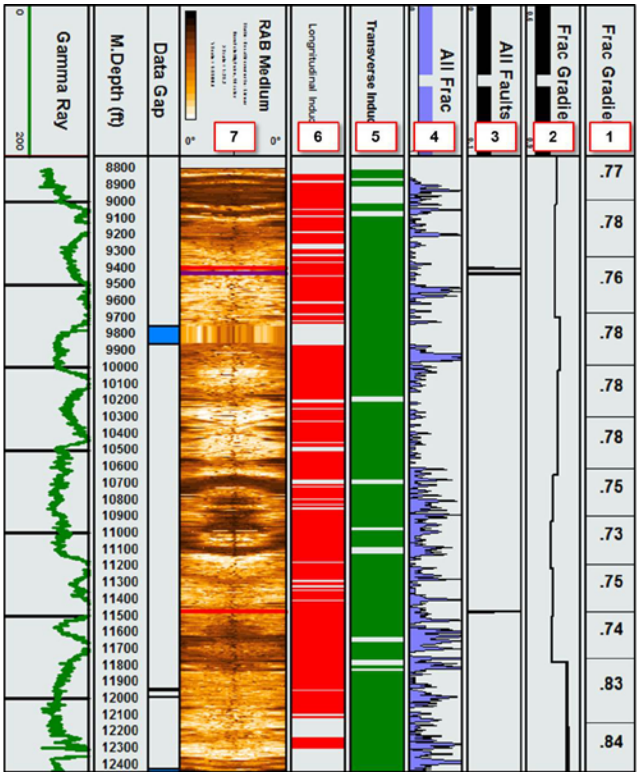

Figure 13: SEM 12H Near-wellbore stress, fracture frequencies and frac gradients.

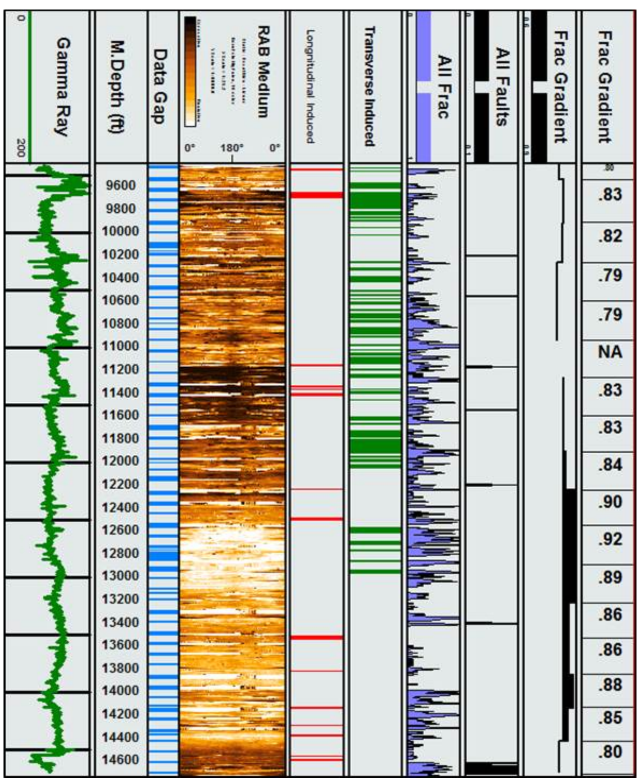

Figure14: TH 2H Near-wellbore stress, fracture frequencies and frac gradients.

average fracture gradient is the lowest observed in the three wells. (Note a comparison of values in Table 1).

TB 2H Near Wellbore Stress

There are fewer longitudinal and transverse fractures present in the TB 2H well (Figure 14) than in the SEM 12H (Figure 13). Toeward of 12,900', there is a marked absence of transverse fractures, indicating relatively higher horizontal stress values. This correlates with the higher fracture gradients observed. The fracture gradient values per stage in the TB 2H range from 0.83 to 0.92. The average fracture gradient is 0.84,which is the highest seen in the 3 laterals. A majority of the fractures in this well strike E-W and are cemented. The low population of fractures aligned with S_{Hmax} may also contribute to the high fracture pressure gradient.

At the toe of the well, we observe a cluster of 9 low-angle faults likely related to nearby thrusting. Geomechanical study determined that the faults at 10,200' and 11,168' are critically stressed. The stage with the fault at 11,168 was not successfully pumped (labelled "NA" in the Frac Gradient track). The fracture gradient is observed to decrease healward of a measured depth of 12,200'. This decrease in fracture gradient is accompanied by an marked increase in the development of transverse induced fractures. The number of critically-stressed fractures also increases healward of 12,900'.

PAL 9H Near Wellbore Stress

In the Pal 9H (Figure 15), the interval from 13,400'-14600' was completed open-hole due to problems running casing. There are many places along the lateral where either longitudinal fractures or transverse fractures are present, but not both. This is the most heavily fractured well observed of the 3 (3,451 fractures). The open fracture population (Track 3), accounts for 24% of the total number of fractures. The open fractures are aligned with S_{Hmax} and exhibit a notable increase in fracture frequency between 11,100'-14,100'. The highest fracture gradients in the Palomino 9H are observed between 10,300'-11,100'. This interval is typified by a scarcity of open fractures and an increase in transverse fractures. Intervals with only transverse induced fractures are usually areas with higher stress anisotropy. There are 16 faults present in the Palomino 9H; 6 of these occur in the open-hole section of the well. The average fracture gradient is 0.80, excluding the most toeward stage which is open hole.

Table 1: Comparison of Features from Borehole Image Analyses with Frac Gradients

Well	# of Fractures	Faults	Longitudinal Induced	Transverse Induced	Average Frac Gradient
Mansfield SE 12H (SEM 12H)	889	3	Abundant	Abundant	0.77
Thoroughbred 2H (TB 2H)	1,330	16	Few	Moderate	0.84
Palomino 9H (Pal 9H)	3,451	16	Moderate	Moderate	0.80

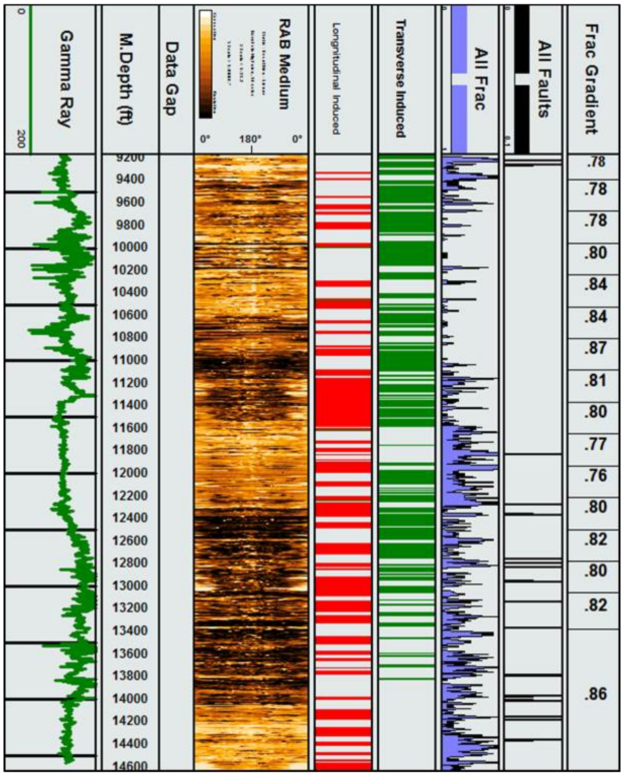

Figure 15: Pal 9H Near-wellbore stress, fracture frequencies and frac gradients.

TH 2H Geomechanical Model & Critically-Stressed Fractures

A full suite of logs available from the pilot hole was used to derive a geomechanical model consisting of horizontal stresses, pore pressure and overburden. The model was calibrated and validated by comparison with drilling events and geomechanical features determined from mud/drilling reports and the interpreted image log. The calibrated model is displayed on the left side of Figure 16.

Averaged properties of the calibrated geomechanical model from the pilot hole were then adapted to the lateral by matching GR signatures between the wellbores, taking into consideration structural shifts (e.g. faults) as reported by the geo-steering report and/or results of the interpreted image. Combination of the projected geomechanical model with the structural characteristics of the interpreted image enabled identification of critically-stressed fractures (CSF's), which are defined as those fractures/faults that are positioned favorably to fail by shear, and hence, are more likely to be conductive. Representation of the CSF's is displayed on the right side of Figure 16.

Barnett Stimulation Results

The SEM 12H and the TB 2H were both logged with lateral borehole image tools. The TB 2H and the SEM 12H were the first two laterals stimulated. At the time, our conclusions of the results of these lateral image logs were not fully formulated. However stimulation designs for subsequent offsetting laterals will incorporate significant modifications based on the results of our analyses of the borehole image logs. The most significant conclusion from this investigation is that the drilling induced fractures mapped in the lateral image logs are a reasonable proxy for expected induced hydraulic fracture behavior. If we detect multi-planar drilling-induced fractures (e.g., both longitudinal and transverse), we can expect a greater propensity for multi-planar induced fracturing which would produce a wide SRV. If we observe single planar drilling induced fractures, (e.g., transverse fractures only), we can expect a greater propensity for single planar fractures, with a narrower SRV. An absence of drilling induced fractures can indicate high compressive stresses. This would indicate a difficulty to initiate fractures and possibly higher fracture gradients.

<u>SEM 12H-</u> The image log data showed both transverse and longitudinal drilling-induced fractures along the entire lateral. The stimulations in this lateral treated with low fracture pressures. All perf clusters seemed to accept fluid, and proppant was easily placed. The flowback and production on this well was exceptional despite rather average petrophysical properties. We can only conclude that the production results were due to superior stimulation effects and large SRV resulting from low, less anisotropically-stressed rock. Subsequent completions, currently ongoing, will benefit from the information gained from the SEM 12H. Fewer (but larger) stages will be required, the number of perf clusters will be increased, the pump rate will be increased, and almost 50% of the proppant volume will be 100 mesh sand.

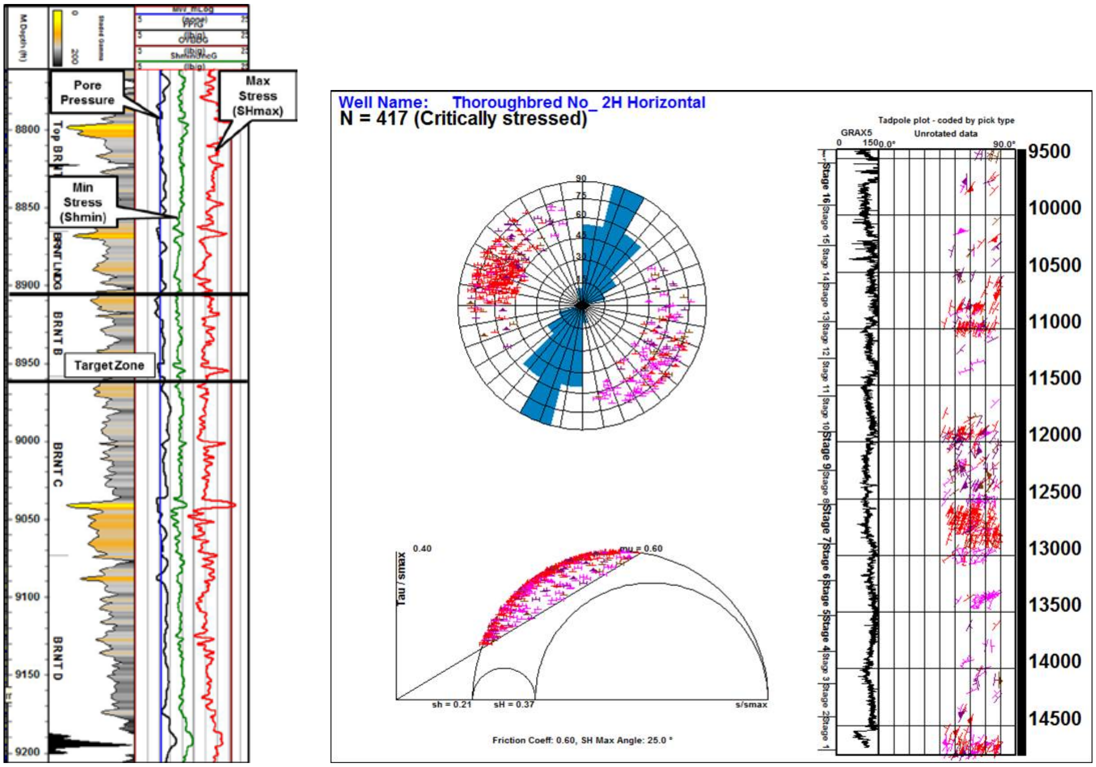

Figure 16: On the left is the geomechanical model for the TH 2H vertical pilot hole with the target zone labeled. On the right is a compound diagram indicating the characteristics of the critically-stressed fracture (CSF) population. There are a large number of CSFs from the fault at 12,900' to ~11,900'. The interval from 10,750' to 11,100' is also characterized by a large increase in CSFs. The frac stage at 11,168 had a high-angle critically-stressed fault and more than 60 critically-stressed fractures. This stage was not successfully pumped.

TB 2H- As described previously, the TB 2H showed relatively few drilling induced fractures in the first 2500' of the lateral. Fracturing in this section showed high stress gradients, and it proved difficult to place proppant. In fact, use of x-linked gel was necessary in several of the stages to place the desired proppant. At about 12,200' TD, the stresses in the lateral apparently changed. The occurrence of drilling induced fractures increased, the fracture stress gradients diminished significantly, and the subsequent stages took proppant much more easily.

Since the TB 2H well was completed, a 250' offset was drilled but 100' lower than the TB 2H into the C bench. While drilling, the mud logger detected the occurrence of frac sand from the TB 2H completion. Figure 17 shows that a high amount of frac sand was mapped in the first 2500' in the lateral then, at approximately 12,200', the frac sand in the offsetting C bench well decreased considerably. Our interpretation is that an increase in the abundance

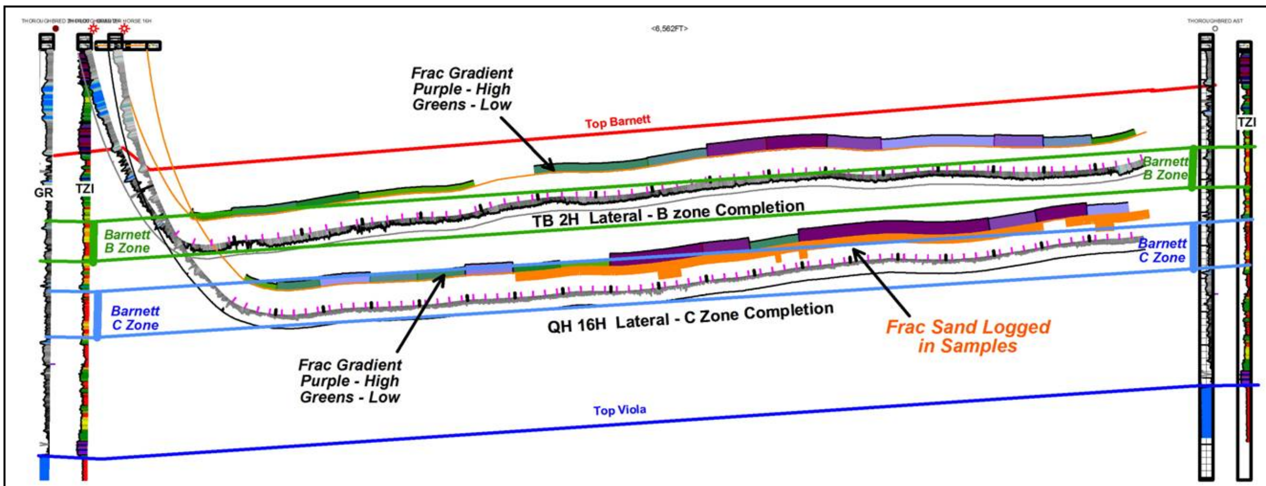

Figure 17: Horizontal cross-section of TB 2H and QH 16H. Wells are 250' apart. QB 16H was drilled after the TB 2H had been hydraulically fractured. Frac gradients are illustrated along with frac sand logged in samples during drilling of the QH 16H lateral.

of planar fracturing occurred in the higher stress toe-section of the lateral. Planar fractures created a much greater focus of fracture energy and, as a result, there was a greater fracture height growth down into the C bench. The lessons learned from the TB 2H data were applied to the newly completed QH 16H well. Stages were added to the toe section of the lateral, the designed stage volume was reduced and the fracture pump rate was reduced by 30%.

Conclusions:

1. Rock Mechanical properties and horizontal stresses determine the nature of complex fracturing in unconventional stimulation. In particular the Poisson's ratio of the rock and the degree of horizontal stress anisotropy are the two key parameters.
    a. In this investigation we have found that the horizontal stress anisotropy is the parameter that exhibits the most variability.
2. Borehole image logs and dipole sonic logs can be useful to predict these key parameters
    a. Our work has demonstrated that drilling induced fractures seen on image logs can be a useful proxy for predicting the nature of complex fracturing
    b. In areas of high stress variability and structural complexity additional horizontal borehole images may need to be run.
3. Knowledge of the nature of complex fracturing can be used to customize stimulation stage design to reduce cost and/or increase the effectiveness of the stimulation. The key parameters that can be adjusted are:
    a. Stage length and volume.
    b. Fracturing pumping rate.
    c. Proppant particle sizing and proportioning.
    d. Fracturing fluid type.

References:

Barnett Shale Maps, 2007: *http://blumtexas.blogspot.com,* Accessed April 2014

Blakey, R., 2005, Paleogeography and geologic evolution of North America: *http://jan.ucc.nau.edu/~rcb7/ RCB.html*, accessed April 2014.

Bowker, K.A., 2007a, Barnett Shale gas production, Fort Worth basin: issues and discussion: American Association Petroleum Geologists Bulletin, v. 91, p. 523–533.

Bruner, K.R., Smosna, R., 2011, A comparative study of the Mississippian Barnett Shale, Fort Worth Basin, and Devonian Marcellus Shale, Appalachian Basin, U.S. Department of Energy, National Energy Technology Laboratory, DOE/NETL -2011/1478

Gale, J.F.W., Reed, R.M., and Holder J., 2007, Natural fractures in the Barnett Shale and their importance for hydraulic fracture treatments: American Association Petroleum Geologists Bulletin, v 91, p. 603–622.

Givens, N., and Zhao, H., 2009, The Barnett shale: not so simple after all: *https://www.republicenergy.com/ Articles/Barnett_Shale/Barnett.aspx*, accessed April 2014

Gutschick, R.C., and Sandberg, C.A., 1983, Mississippian continental margins of the conterminous United States, *in* Stanley, D.J., and Moore, G.T., eds., The shelf break margin—critical interface on continental margins,: Society of Economic Paleontologists and Mineralogists, Special Publication 33, p. 79–96.

Henry, J.D., 1982, Stratigraphy of the Barnett Shale (Mississippian) and associated reefs in the northern Fort Worth basin, *in* Martin, C.A., ed., Petroleum geology of the Fort Worth basin and Bend Arch area: Dallas Geological Society, p. 157–178.

Hickey, J.J. and Henk, B., 2007, Lithofacies summary of the Mississippian Barnett Shale, Mitchell 2 T.P. Sims well, Wise County, Tx: American Association Petroleum Geologists Bulletin, v. 91, p. 437–443.

Hill, R.J., Jarvie, D.M., Zumberge, J., Henry, M., and Pollastro, R.M., 2007a, Oil and gas geochemistry and petroleum systems of the Fort Worth Basin: American Assocociation Petroleum Geologists Bulletin, v. 91, p. 445–473.

Hill, R.J., Zhang, E., Katz, B.J., and Tang, Y., 2007b, Modeling of gas generation from the Barnett Shale, Fort Worth Basin, Texas: American Association Petroleum Geologists Bulletin, v. 91, p. 501–521.

Jarvie, D.M., Hill, R.J., Ruble, T.E., and Pollastro, R.M., 2007, Unconventional shale-gas systems: the Mississippian Barnett Shale of north-central Texas as one model for thermogenic shale-gas assessment: American Association Petroleum Geologists Bulletin, v. 91, p. 475–499

Ketter, A.A., 2008 A field study optimizing completion strategies for fracture initiation in Barnett Shale horizontal wells, SPE Annual Technical Conference, San Antonio, TX, USA

Loucks, R.G., and Ruppel, S.C., 2007, Mississippian Barnett Shale: lithofacies and depositional setting of a deep-water shale-gas succession in the Fort Worth Basin, Texas: American Association Petroleum Geologists Bulletin, v. 91, p. 579–601.

Martineau, D.F., 2007, History of the Newark East field and the Barnett Shale as a gas reservoir, American Association Petroleum Geologists Bulletin, v. 91, p. 399–403.

Montgomery, S.L., Jarvie, D.M., Bowker, K.A., and Pollastro, R.M., 2005, Mississippian Barnett Shale, Fort Worth basin, north-central Texas: Gas-shale play with multi-million cubic foot potential: American Association Petroleum Geologists Bulletin, v. 89, p. 155–175.

Olsen, T.N., Bratton, T.R. Thiercelin, M.J., 2009, Quantifying proppant transport for complex fractures in unconventional reservoirs. SPE Hydraulic Fracturing Technology Conference, The Woodlands, TX, USA

Papazis, P.K., 2005, Petrographic characterization of the Barnett Shale, Fort Worth Basin, Texas: M.S. thesis, University of Texas at Austin Austin, Texas, 142 p, and appendices.

Pollastro, R.M., 2007, Total petroleum system assessment of undiscovered resources in the giant Barnett Shale continuous (unconventional) gas accumulation, Fort Worth Basin, Texas: American Association Petroleum Geologists Bulletin, v. 91, p. 551–578.

Pollastro, R.M., Hill, R.J., Jarvie, D.M., and Henry, M.E., 2003, Assessing undiscovered resources of the Barnett-Paleozoic total petroleum system, Bend Arch-Fort Worth basin province, Texas: *http://www.searchanddiscovery.net/documents/pollastro/images/article.pdf*, assessed April 2014.

Slatt, R., Singh, P., Borges, G., Perez, R., Portas, R., Vellejo, J., Ammerman, M., Coffey, W., and Eslinger, E., 2009, Reservoir characterization of unconventional gas shales: example from the Barnett Shale, Texas, U.S.A.: Search and Discovery Article #30075, *http://www.searchanddiscovery.net/documents/2009/30075slatt/ndx_slatt.pdf*, accessed April 2014

Warpinski, N.R., Kramm, R.C., Heinze, J.R., Waltman , C.K. , 2005, Comparison is single and dual-array microseismic mapping techniques in the Barnett Shale, SPE Conference Paper 95568-MS

Warpinski, N.R., Teufel, L.W, 1987, Influence of geological discontinuities on hydraulic fracture propagation, JPT February, 1987, Pg 209-220

Waters, G., Schlumberger, J., Jackson, R., Ketter, A., et al., 2006, Use of Horizontal Well Image Tools to Optimize Barnett Shale reservoir exploitation, SPE 103202